SCIENCE CHINA
Information Sciences

• LETTER •
Special Focus on High-Resolution Radar

April 2019, Vol. 62 040306:1–040306:3
https://doi.org/10.1007/s11432-018-9736-9

A radar waveform bandwidth selection strategy for wideband tracking

Shaoqiang CHANG[1], Honggang ZHANG[2], Teng LONG[1*],
Quanhua LIU[1,3] & Le ZHENG[4]

[1]Radar Research Laboratory, School of Information and Electronics, Beijing Institute of Technology, Beijing 100081, China;
[2]Department of Electronic Engineering, Tsinghua University, Beijing 100084, China;
[3]Key Laboratory of Electronic and Information Technology in Satellite Navigation (Beijing Institute of Technology), Ministry of Education, Beijing 100081, China;
[4]Electrical Engineering Department, Columbia University, New York NY 10027, USA

Received 13 October 2018/Accepted 6 December 2018/Published online 4 March 2019

Citation Chang S Q, Zhang H G, Long T, et al. A radar waveform bandwidth selection strategy for wideband tracking. Sci China Inf Sci, 2019, 62(4): 040306, https://doi.org/10.1007/s11432-018-9736-9

Dear editor,

The performance of radar target detection and tracking is greatly influenced by waveform bandwidth. Ref. [1] proposes that very narrowband waveforms are usually employed for search, narrowband waveforms are used for tracking, and wideband waveforms are used for classification. Ref. [2] considers that ballistic missiles may impose the challenge of closely space objects (CSO), and tracking in a CSO environment may motivate high-resolution tracking waveforms to ensure firm tracks on individual objects. Thus, according to practical requirements, narrowband and wideband waveforms are employed for target cued search/acquisition and stable tracking, respectively [3].

A key problem evolves, namely, when and how to switch from narrowband acquisition to wideband tracking. Because the range measurement accuracy is not high for target acquisition, the narrowband range gate is relatively large. At this point, switching to wideband waveforms directly, increasing range resolution cells and false alarm numbers will decrease the track filtering accuracy or even lose the track. Ref. [4] studied the problem of adaptive waveform selection for target tracking by a multistatic radar system based on minimizing the tracking mean square error. The waveform selection for maneuvering targets within an interacting multiple model (IMM) framework was studied in [5]. However, neither waveform selection criteria discussed the bandwidth transition from narrowband to wideband.

In this study, we focus on the analyses of waveform bandwidth selection strategy for transition from target narrowband acquisition to wideband stable tracking. A novel waveform design method is proposed to gradually increase the signal bandwidth on the premise of the constant tracking error caused by a false alarm so that the system can quickly and smoothly switch from the narrowband acquisition to the stable wideband tracking state.

Bandwidth gradual-transition waveform design method. Generally, it is assumed that the Kalman filtering [6] algorithm is adopted in radar. If the target state prediction vector and state prediction covariance matrix of the k-th time are $\hat{\boldsymbol{X}}(k|k-1)$ and $\boldsymbol{P}(k|k-1)$, respectively, then the updated state vector and state covariance matrix of the k-th time are shown in (1) and (2):

$$\hat{\boldsymbol{X}}(k|k) = \hat{\boldsymbol{X}}(k|k-1) + \boldsymbol{K}(k)\boldsymbol{v}(k), \qquad (1)$$

$$\boldsymbol{P}(k|k) = \boldsymbol{P}(k|k-1) - \boldsymbol{K}(k)\boldsymbol{S}(k)\boldsymbol{K}^{\mathrm{T}}(k), \qquad (2)$$

where $\boldsymbol{K}(k)$ is the filter gain matrix, $\boldsymbol{v}(k)$ is the measurement residual and $\boldsymbol{S}(k)$ is the measure-

* Corresponding author (email: longteng@bit.edu.cn)

ment prediction covariance matrix. The area (volume) of an n_z-dimension elliptical (ellipsoidal) tracking range gate [7] is $V(n_z) = c_{n_z}\gamma^{\frac{n_z}{2}}|\boldsymbol{S}(k)|^{\frac{1}{2}}$. γ is the tracking range gate parameter which satisfies $\boldsymbol{v}^{\mathrm{T}}(k)\boldsymbol{S}^{-1}(k)\boldsymbol{v}(k) \leqslant \gamma$. The c_{n_z} is 2 for radar measurement range tracking gate (1 dimension). Thus, the area of a radar measurement range tracking gate is $V_1(k) = 2\gamma^{\frac{1}{2}}S_{11}(k)^{\frac{1}{2}}$ in the k-th time. $S_{11}(k)$ is the first element on the diagonal of matrix $\boldsymbol{S}(k)$.

If n pulses are accumulated, the average false alarm number in tracking range gate is $N(k) = 8\gamma^{\frac{1}{2}}S_{11}(k)^{\frac{1}{2}}nBP_{\mathrm{fa}}/\mathrm{c}$ for the k-th time, where c is the speed of light, B is the signal bandwidth, P_{fa} is the probability of false alarm. Obviously, a larger bandwidth will increase the false alarm numbers in the tracking range gate. On the other hand, measurement prediction is also related to the signal bandwidth. Assume that the radar adopts linear frequency modulation (LFM) ranging and employs monopulse techniques to measure the angles (targets near the axis); the root mean square error (RMSE) of range and angle measurement [8, 9] are $e_r = \sqrt{3}\mathrm{c}/(2\pi B\sqrt{2\mathrm{SNR}})$ and $e_\theta \approx \theta_{3\,\mathrm{dB}}/(K_\theta\sqrt{2n\mathrm{SNR}})$, respectively, where K_θ is the monopulse slope ($K_\theta = 1.4$ in this study). n is number of independent measurements smoothed by the tracking filter and $\theta_{3\,\mathrm{dB}}$ is 3 dB beamwidth of radar. The SNR is the echo signal-to-noise ratio. If there is a false alarm in range gate, then the target state estimate vector can be updated as

$$\begin{aligned}&\hat{\boldsymbol{X}}(k|k)\\&=\hat{\boldsymbol{X}}(k|k-1)+\boldsymbol{K}(k)(\alpha\boldsymbol{v}(k)+(1-\alpha)\boldsymbol{v}_f(k)),\end{aligned}\tag{3}$$

where $\boldsymbol{v}_f(k)$ is the measurement residual corresponding to a false alarm and α is the observation weight of real target. Because the false alarm is uniformly distributed in the tracking range gate, thus, $\mathrm{E}[\boldsymbol{v}_f(k)\boldsymbol{v}_{\boldsymbol{f}}^{\mathrm{T}}(k)] = \mu\boldsymbol{S}(k)$, where $\mathrm{E}[\cdot]$ is statistical average calculation function and μ is a constant.

According to (3) and [7], the state covariance matrix can be updated as

$$\begin{aligned}&\boldsymbol{P}'(k|k)\\&=\mathrm{E}\left\{\left[\hat{\boldsymbol{X}}(k|k)-\boldsymbol{X}(k)\right]\left[\hat{\boldsymbol{X}}(k|k)-\boldsymbol{X}(k)\right]^{\mathrm{T}}\right\}\\&=\boldsymbol{P}(k|k-1)-(2\alpha-\alpha^2)\boldsymbol{K}(k)\boldsymbol{S}(k)\boldsymbol{K}^{\mathrm{T}}(k)\\&\quad+(1-\alpha)^2\mu\boldsymbol{K}(k)\boldsymbol{S}(k)\boldsymbol{K}^{\mathrm{T}}(k)\\&=\boldsymbol{P}(k|k-1)-\boldsymbol{K}(k)\boldsymbol{S}(k)\boldsymbol{K}^{\mathrm{T}}(k)+[1-(2\alpha-\alpha^2)\\&\quad+(1-\alpha)^2\mu]\boldsymbol{K}(k)\boldsymbol{S}(k)\boldsymbol{K}^{\mathrm{T}}(k),\end{aligned}\tag{4}$$

where $\boldsymbol{X}(k)$ is the real motion state of target. If $1-y = 1-(2\alpha-\alpha^2)+(1-\alpha)^2\mu$, then $1-y$ represents the effect of a false alarm on tracking performance under the normalized measurement prediction covariance and gain condition. And the value of y is between 0 and 1. Considering that there may be more than one false alarm number, (4) can be rewritten as

$$\begin{aligned}\boldsymbol{P}'(k|k)&=\boldsymbol{P}(k|k-1)-\boldsymbol{K}(k)\boldsymbol{S}(k)\boldsymbol{K}^{\mathrm{T}}(k)\\&\quad+(1-y)N(k)\boldsymbol{K}(k)\boldsymbol{S}(k)\boldsymbol{K}^{\mathrm{T}}(k).\end{aligned}\tag{5}$$

Because the false alarm number in normal working scenarios of tracking radar is suppressed very low, $N(k)$ is usually much less than 1. Obviously, a false alarm has no effect on the $\boldsymbol{P}(k|k-1)$, but will change the influence of $\boldsymbol{K}(k)\boldsymbol{S}(k)\boldsymbol{K}^{\mathrm{T}}(k)$ to $\boldsymbol{P}'(k|k)$.

According to (5), the effect of false alarm on tracking performance is related to $1-y$, $\boldsymbol{K}(k)\boldsymbol{S}(k)\boldsymbol{K}^{\mathrm{T}}(k)$ and $N(k)$. $1-y$ is a constant, $\boldsymbol{K}(k)\boldsymbol{S}(k)\boldsymbol{K}^{\mathrm{T}}(k)$ will change over time; thus, the effect of false alarm evolves at different times. The increase in the tracking error caused by the unit false alarm can be defined as

$$\begin{aligned}\beta&=(1-y)\mathrm{trace}\big(\boldsymbol{M}\boldsymbol{K}(k)\boldsymbol{S}(k)\boldsymbol{K}^{\mathrm{T}}(k)\boldsymbol{M}^{\mathrm{T}}\big)\\&=(1-y)\beta',\end{aligned}\tag{6}$$

where $\boldsymbol{M}$ is the weighted matrix used to adjust the weighted value of the different dimensional tracking error. Generally, $\boldsymbol{M}$ can be taken as

$$\boldsymbol{M}=\begin{bmatrix}1&0&0&0&0&0\\0&0&1&0&0&0\\0&0&0&0&1&0\end{bmatrix}.\tag{7}$$

According to (5) and (6), the tracking error caused by false alarm can be constant if $\boldsymbol{U}(k) = \beta' N(k) = \mathrm{trace}(\boldsymbol{M}\boldsymbol{K}(k)\boldsymbol{S}(k)\boldsymbol{K}^{\mathrm{T}}(k)\boldsymbol{M}^{\mathrm{T}})N(k)$ remains consistent during tracking. Therefore, the bandwidth gradual-transition waveform design method can be demonstrated as follows.

(1) Initialize the track vector and matrix ($k = 0$). Predict the motion state vector $\hat{\boldsymbol{X}}(1|0)$, state prediction covariance $\boldsymbol{P}(1|0)$, measurement prediction covariance $\boldsymbol{S}(1)$ and gain matrix $\boldsymbol{K}(1)$ of the next moment $k = 1$.

(2) Calculate the average false alarm number $N(1) = 8\gamma^{\frac{1}{2}}S_{11}(1)^{\frac{1}{2}}nBP_{\mathrm{fa}}/\mathrm{c}$ and $\boldsymbol{U}(1) = \mathrm{trace}(\boldsymbol{M}\boldsymbol{K}(1)\boldsymbol{S}(1)\boldsymbol{K}^{\mathrm{T}}(1)\boldsymbol{M}^{\mathrm{T}})N(1)$.

(3) Update the state estimate vector $\hat{\boldsymbol{X}}(k|k)$ and state covariance matrix $\boldsymbol{P}(k|k)$ of k-th time.

(4) Predict the state vector $\hat{\boldsymbol{X}}(k+1|k)$, state prediction covariance $\boldsymbol{P}(k+1|k)$, measurement prediction covariance $\boldsymbol{S}(k+1)$ and gain matrix $\boldsymbol{K}(k+1)$ of next moment $k+1$.

(5) Take the $\boldsymbol{U}(k) = \boldsymbol{U}(1)$ and calculate false alarm number $N(k) = \boldsymbol{U}(k)/\mathrm{trace}(\boldsymbol{M}\boldsymbol{K}(k)$ $\boldsymbol{S}(k)\boldsymbol{K}^{\mathrm{T}}(k)\boldsymbol{M}^{\mathrm{T}})$ for k-th time.

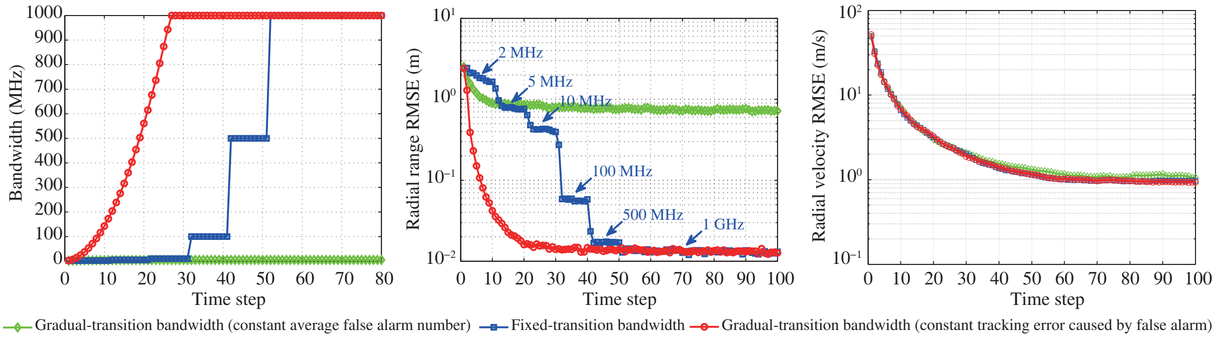

(a) (b) (c)

Figure 1 (Color online) Bandwidth design results and measurement filtering RMSE for different methods. (a) Bandwidth design results; (b) radial range filtering RMSE; (c) radial velocity filtering RMSE.

(6) According to $N(k)$, design the waveform bandwidth of the k-th time as $B(k) = N(k)c/8\gamma^{\frac{1}{2}}S_{11}(k)^{\frac{1}{2}}nP_{\rm fa}$.

(7) $k = k + 1$ and return to (3).

Simulation and analysis. We present a simulation example for the proposed method. In this example, the tracking data rate is set to 0.5 s. The SNR is 20 dB, and the radar beamwidth is 0.08°. $P_{\rm fa}$ is 1×10^{-7}, and γ is 16. The pulse accumulation number n is 1. The initialized tracking bandwidth is 2 MHz, and the final ideal bandwidth is 1 GHz. The target motion state is $\hat{\boldsymbol{X}}(0|0) = [x\ v_x\ y\ v_y\ z\ v_z]$, where $[x\ y\ z] = [-1.2398 \times 10^6\ \ -9.9801 \times 10^5\ \ 1.6614 \times 10^6]$ m is the position of the target in rectangular coordinate system and $[v_x\ v_y\ v_z] = [2.1261 \times 10^3\ 4.0840 \times 10^3\ \ -2.7719 \times 10^3]$ m/s is the target velocity in the corresponding direction.

To demonstrate the superiority of the proposed method, the comparison results of another gradual-transition bandwidth (keep average false alarm number constant) and fixed-transition bandwidth method are presented in the simulation. The order of the fixed-transition bandwidth is 2, 5, 10, 100, 500 MHz, and 1 GHz. And the filtering time of each fixed bandwidth frequency is set as 10 steps. Figure 1 shows the bandwidth design result, radial range and velocity measurement filtering RMSE for three methods. The final convergent result of gradual-transition bandwidth (keep average false alarm number constant) is stable at 5 MHz. It is observed that the method we proposed, gradual-transition bandwidth (keep tracking error caused by false alarm constant), can make the bandwidth transition more rapidly and smoothly compared with the other two methods. On the other hand, the tracking accuracy can also be rapidly improved.

Conclusion. A radar waveform bandwidth selection strategy for wideband tracking is presented in this study. A theoretical analysis shows that the bandwidth gradual-transition waveform selection method can restrain the effect of the false alarm number with increasing waveform bandwidth and keep the tracking error caused by false alarm constant to ensure that the track is not lost. Moreover, the radar system can rapidly and smoothly transit from the narrowband acquisition scenarios to the wideband stable tracking scenarios, which is beneficial to target recognition. The simulation results also demonstrate the effectiveness and superiority of the proposed method.

Acknowledgements This work was supported by Chang Jiang Scholars Program of China (Grant No. T2012122), Programme of Introducing Talents of Discipline to Universities (111 Project) (Grant No. B14010), and National Natural Science Foundation of China (Grant No. 61771050).

References

1 Thomas J. Phased-Array Radar Design: Application of Radar Fundamentals. Raleigh: SciTech Pub Inc, 2009
2 William L M, James A S. Principles of Modern Radar: Radar Applications. Raleigh: SciTech Pub Inc, 2014
3 Roth K R, Austin M E, Frediani D J, et al. The Kiernan reentry measurements system on kwajalein atoll. Lincoln Lab J, 1989, 2: 247–276
4 Nguyen N, Dogancay K, Davis L. Adaptive waveform selection for multistatic target tracking. IEEE Trans Aerosp Electron Syst, 2015, 51: 688–701
5 Savage C O, Moran B. Waveform selection for maneuvering targets within an IMM framework. IEEE Trans Aerosp Electron Syst, 2007, 43: 1205–1214
6 Park S T, Lee J G. Improved Kalman filter design for three-dimensional radar tracking. IEEE Trans Aerosp Electron Syst, 2001, 37: 727–739
7 He Y, Xiu J J, Guan X, et al. Radar Data Processing with Application. 3rd ed. Beijing: Publishing House of Electronics Industry, 2013
8 Skolnik M L. Introduction to Radar Systems. 3rd ed. Boston: McGraw Hill, 2001
9 Sherman S M, Barton D K. Monopulse Principles and Techniques. 2nd ed. Boston: Artech House, 2011